Science of the Total Environment xxx (2016) xxx–xxx

Contents lists available at ScienceDirect

Science of the Total Environment

journal homepage: www.elsevier.com/locate/scitotenv

Surface energy balance of an extensive green roof as quantified by full year eddy-covariance measurements

Jannik Heusinger *, Stephan Weber

Climatology and Environmental Meteorology, Institute of Geoecology, TU Braunschweig, Langer Kamp 19c, Braunschweig, Germany

HIGHLIGHTS

- First eddy-covariance measurements on extensive green roof
- Analysis of surface energy balance during dry and wet periods
- High daytime Bowen ratios prevailed during warm, dry periods.
- Green roof revealed significant nocturnal cooling potential.
- Maximum daily evapotranspiration ration of green roof was 3.3 mm.

GRAPHICAL ABSTRACT

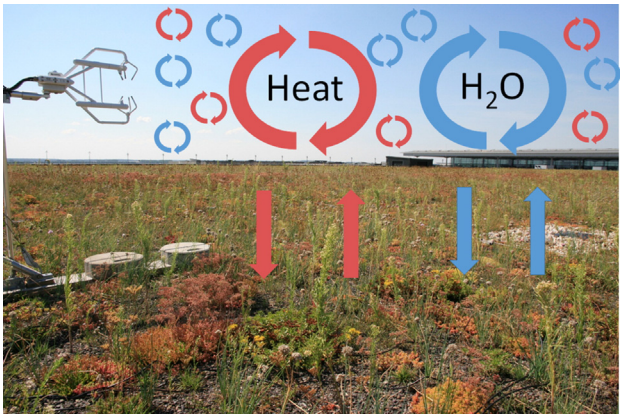

ARTICLE INFO

Article history:
Received 12 August 2016
Received in revised form 20 October 2016
Accepted 21 October 2016
Available online xxxx

Editor: Elena PAOLETTI

Keywords:
Bowen ratio
Evapotranspiration
Green infrastructure
Extensive roof greening
Leaf area

ABSTRACT

Green roofs are discussed as a promising type of green infrastructure to lower heat stress in cities. In order to enhance evaporative cooling, green roofs should ideally have similar Bowen ratio (β = sensible heat flux/latent heat flux) characteristics such as rural sites, especially during summer periods with high air temperatures. We use the eddy-covariance (EC) method to quantify the energy balance of an 8600 m^2 extensive, non-irrigated green roof at the Berlin Brandenburg Airport, Germany over a full annual cycle. To understand the influence of water availability on green roof-atmosphere energy exchange, we studied dry and wet periods and looked into functional relationships between leaf area, volumetric water content (VWC) of the substrate, shortwave radiation and β. The surface energy balance was dominated by turbulent heat fluxes in comparison to conductive substrate heat fluxes. The Bowen ratio was slightly below unity on average but highly variable due to ambient meteorology and substrate water availability, i.e. β increased to 2 in the summer season. During dry periods mean daytime β was 3, which is comparable to typical values of urban instead of rural sites. In contrast, mean daytime β was 0.3 during wet periods. Following a summer wet period the green roof maximum daily evapotranspiration (ET) was 3.3 mm, which is a threefold increase with respect to the mean summer ET. A multiple regression model indicated that the substrate VWC at the present site has to be >0.11 $m^3\ m^{-3}$ during summer high insolation periods (>500 W m^{-2}) in order to maintain favourable green roof energy partitioning, i.e. mid-day $\beta < 1$. The microclimate benefit of urban green roofs can be significantly optimised by using sustainable irrigation approaches.

* Corresponding author.
E-mail address: j.heusinger@tu-braunschweig.de (J. Heusinger).

http://dx.doi.org/10.1016/j.scitotenv.2016.10.168
0048-9697/

1. Introduction

Urban green roofs and green infrastructure provide a number of ecosystem services, such as microclimate regulation, air purification, carbon sequestration, storm water retention, and increase of biodiversity (Oberndorfer et al., 2007; Coutts and Hahn, 2015; Gómez-Baggethun et al., 2013). Recently, a growing number of studies assessed and evaluated ecosystem services of urban green across cities in different cultures and climate zones (e.g. Derkzen et al., 2015; Haase et al., 2014). Green infrastructure is particularly important in reducing excess heat in cities (Bowler et al., 2010). This is of specific interest during periods of increased temperatures, i.e. hot summer conditions and heat waves. The need to reduce urban heat stress is urgent, given ongoing climate change with an increasing frequency of heat waves (e.g. Mazdiyasni and AghaKouchak, 2015; Russo et al., 2014).

Urban excess heat, e.g. the urban heat island, is a result of the three-dimensional urban fabric with a higher fraction of sealed surfaces, increased surface runoff and less vegetated areas compared to the rural environment (Oke, 1982). Consequently, the urban area experiences a modified surface energy balance and heat storage characteristics. The urban energy balance is dominated by sensible heat fluxes (Q_H) in comparison to latent heat fluxes (Q_E) during daytime, which results in Bowen ratios ($\beta = Q_H/Q_E$) larger than unity. Typical average urban β can reach daytime values of 1.4 in Oberhausen, Germany (Goldbach and Kuttler, 2013), 2.6 in Basel, Switzerland (Christen and Vogt, 2004), 4.4 in Marseille, France (Grimmond et al., 2004), and 5 in Phoenix, USA or Melbourne, Australia (Chow et al., 2014; Coutts et al., 2007).

Vegetation density in cities is negatively correlated with β due to the stronger effect of evaporative cooling with increased surface green fractions (Grimmond and Oke, 2002; Christen and Vogt, 2004). The implementation of roof greening is one promising way to enhance vegetation density in cities. Taking Germany as example, green roofs cover an average area of 1.4×10^6 m^2 (1.5 m^2 per capita) in the cities of Munich, Karlsruhe and Stuttgart (Ansel et al., 2015). Increasing urban green density on rooftops has the advantage that this strategy is not in space competition with the surface built environment, in contrast to other types of greening, e.g. urban parks. Green roofs are defined into extensive and intensive types. Intensive green roofs consist of herbaceous plants, shrubs and single trees, making irrigation and large substrate depths necessary (Pfoser et al., 2014). The extensive type consists of mosses, *Sedum* species and herbaceous plants, which are not considered to need irrigation for survival. Typically, substrate depths of extensive roofs are between 0.02 m and 0.15 m (Berndtsson, 2010). Currently, >90% of green roofs in Germany are extensive and non-irrigated (Zinco GmbH and Optigrün international AG, pers. communication).

Green roofs show positive characteristics considering their UHI mitigation potential (Smith and Roebber, 2011), air quality aspects (Yang et al., 2008), retention performance (Stovin et al., 2013) and energy consumption of buildings (Sailor et al., 2011). However, in order to lower warming of cities by evaporative cooling, green roofs ideally should have similar β characteristics such as rural sites (i.e. $\beta \ll 1$), especially during hot periods. We hypothesise that non-irrigated, extensive green roofs show unfavourable heat flux partitioning due to low substrate water availability during hot summer conditions and rainless periods. Hence, green roofs may lose their positive effects on local climate, i.e. evaporative cooling. Tabares-Velasco and Srebric (2011) measured a decrease of Q_E with declining substrate moisture in laboratory green roof experiments whereas Q_H increased. Consequently, the Bowen ratio is affected. Coutts et al. (2013) measured Bowen ratios >4 on a green roof that dropped to <1 after irrigation.

Although green roof models are available (e.g. Kumar and Kaushik, 2005; Sailor, 2008), a lack of validation data is evident (Sailor, 2008). This especially holds for the green roof energy exchange as a function of various meteorological conditions. To the knowledge of the authors, direct measurements of the complete energy balance of green roofs have not been published, yet. Up to now, only individual terms of the green roof energy balance, e.g. evapotranspiration and latent heat fluxes were quantified (e.g. Ayata et al., 2011; Coutts et al., 2013; DiGiovanni et al., 2012; Marasco et al., 2015; Sherrard and Jacobs, 2011; Tabares-Velasco and Srebric, 2011; Voyde et al., 2010; Wolf and Lundholm, 2008). Rates of evapotranspiration were estimated by lysimetry, chamber measurements, substrate heat flux measurements combined with meteorological measurements, and laboratory experiments. In the cited studies at least one term of the energy balance was calculated as a residual or needed to be parameterized.

In this study, we use the state-of-the-art micrometeorological approach to measure surface-atmosphere exchange, i.e. the eddy-covariance (EC) method (Baldocchi, 2014). The advantage of the EC method is that it is a direct method to quantify turbulent exchange of heat and mass without assumptions about the turbulent state of the atmosphere (Lee et al., 2006). The motivation of the present study is to analyse heat flux partitioning of an extensive green roof by surface energy balance measurements over a full annual cycle. We studied dry and wet periods and looked into functional relationships between leaf area, substrate water content, shortwave radiation and β to understand the influence of these variables on green roof-atmosphere energy exchange and heat flux partitioning.

2. Material and methods

2.1. Study area and study period

The green roof is situated on top of a multi-storey car park at the Berlin Brandenburg airport (BER), Germany. The car park is built of a porous mesh façade and a flat roof. The height of the car park is 18 m, which roughly equals the mean building height at the airport. The green roof has a size of about 8600 m^2 and was constructed in May 2012.

The vegetation of the non-irrigated extensive green roof is dominated by *Sedum* species and complemented by herbaceous plants (e.g. *Allium schoenoprasum*, *Trifolium* sp., Fig. 1). The vegetation height varies between 0.1 and 0.3 m. Similar to other green roofs our study site is not completely covered by plants (cf. Section 2.2). The substrate has a depth of 0.09 m and is a homogeneous mix composed of expanded shale, pumice and compost (substrate type “M-leicht”, manufactured by Optigrün AG). Substrate laboratory analysis was conducted to determine substrate parameters not specified in the manufacturer datasheet (Table 1). The green roof substrate is followed by a 3 mm protection mat, a 50 mm insulation layer, and a 160 mm layer of ferroconcrete. The roof has a slope of 2%. Gardeners maintain the roof approximately

Fig. 1. The BER green roof in the summer period showing parts of the eddy covariance setup (sonic anemometer and open-path gas analyser). The photograph was taken on 22 July 2014. (For interpretation of the references to colour in this figure legend, the reader is referred to the web version of this article.)

Please cite this article as: Heusinger, J., Weber, S., Surface energy balance of an extensive green roof as quantified by full year eddy-covariance measurements, Sci Total Environ (2016), http://dx.doi.org/10.1016/j.scitotenv.2016.10.168

Table 1
Substrate parameters as given in the data sheet provided by the substrate/plants supplier (Optigrün AG) as well as determined by laboratory analysis (in italics, average value of 2 samples).

Substrate parameters	Value
Dry bulk density (g cm^{-3})	*0.78*
Bulk density at water saturation (g cm^{-3})	1.22
Maximum volumetric water content (%)	42.3
Porosity (%)	*71*
Organic substance (g l^{-1})	25

every 12 months to harvest undesired plants (mainly herbaceous plants).

The measurement campaign started on 01 July 2014 and lasted until 31 August 2015. The measurements covered a period of 14 months to include the full meteorological summer season in 2015 (June, July, and August) for analysis of dry and wet periods and functional relationships. However, unless explicitly stated in the following, energy exchange will be presented for one full annual cycle, i.e. the twelve-month period from 01 September 2014 to 31 August 2015 (referred to as study period).

2.2. Monitoring leaf area index and vegetation coverage

The green roof surface energy balance is influenced by the amount of green roof biomass, usually parameterized by the leaf area index (LAI). LAI was monitored weekly between 15 April and 31 August 2015 by capturing the variation of the green chromatic information (green fraction) in the RGB space of photographs taken at 10 different, randomly selected roof locations (Fig. S1 in supplementary material). At the end of the measurement period, plant material samples from 17 locations (each 0.1 m^2) were analysed to determine the one-sided leaf area of green leafs per m^2 roof surface (gLAI). Green leaves were considered exclusively, since only these were assumed to be photosynthetically active and transpiring in contrast to yellow, brown or red (*Sedum* sp.) leaves. The green fraction was calculated from photographs taken from the sample locations before harvesting to establish a regression function with gLAI. We calculated green fraction according to the method as proposed by Richardson et al. (2007).

Vegetation coverage, i.e. the surface fraction covered by leaves per m^2 roof surface, was estimated taking the photographs as input to a colour thresholding algorithm in Matlab R2014b. For each photograph, a coverage value was determined and the average for all locations calculated. In contrast to gLAI, yellow and red leaves were also taken into account to calculate vegetation coverage.

2.3. Instrumentation and data handling

The EC setup consisted of an ultrasonic 3D anemometer (CSAT3A, Campbell Scientific, USA) and an open-path infrared gas analyser (EC150, Campbell Scientific, USA) to measure Q_H (W m^{-2}), Q_E (W m^{-2}), and CO_2 flux densities with 10 Hz time resolution at a height of 1.15 m above roof level (arl). The ultrasonic anemometer head was orientated towards SW (= 225°). Results of the analysis of green roof surface-atmosphere exchange of CO_2 will be subject to future publication.

Up- and downward short- and longwave radiation fluxes were measured with a NR01 sensor (Hukseflux, Netherlands). This study defines positive energy fluxes when directed away from the green roof surface, i.e. into the atmosphere or into the roof. Negative fluxes are directed towards the roof surface.

Air temperature and relative humidity were measured at 2 m arl with a HMP155 (Vaisala, Finland) and precipitation with a tipping bucket (Adolf Thies, Germany). Volumetric water content (VWC) and temperature of the substrate were estimated by four sensors (5TM, Decagon Inc., USA) at depths of 0.025 m (1×), 0.05 m (2×) and 0.075 m (1×). A mean value from the three measurements depths was calculated to quantify VWC and is used in the remainder of the paper. The station was further equipped with a leaf wetness sensor (Decagon Inc.) to monitor surface wetness.

The ground heat flux density at the substrate surface (Q_G in W m^{-2}) was calculated from a self-calibrating heat flux plate (HFP01SC, Hukseflux, Netherlands) installed at a depth of 0.05 m ($Q_{G\ HFP}$). Heat storage (ΔQ_S) between surface and heat flux plate was calculated by the calorimetric method and temperature data measured at depths of 0.01 m and 0.03 m according to (Liebethal et al., 2005; Weber, 2006):

$$Q_S = \frac{\Delta T_{substrate}}{\Delta t} * C_s * \Delta z \quad (1)$$

where $\Delta T_{substrate}$ is the difference between two consecutive 30 min averages of the mean substrate temperature above the heat flux plate (K), Δz is the substrate depth (m) at which the heat flux plate was installed and Δt is the time difference between two consecutive 30 min averages (s).

The volumetric heat capacity of the substrate (C_s) was calculated using (Garratt, 1992):

$$C_s = (1-Pv) * \rho_s * C_{ds} + \theta * \rho_w * C_w + (Pv-\theta) * \rho_a * C_a \quad (2)$$

where Pv is the substrate porosity (0.7 $m^3\ m^{-3}$), ρ_s is dry substrate density (780 kg m^{-3}), C_{ds} is specific heat capacity of dry substrate (1027 J $kg^{-1}\ K^{-1}$, Sailor et al., 2008), θ is volumetric water content ($m^3\ m^{-3}$), ρ_w is density of water (1000 kg m^{-3}), C_w is specific heat capacity of water (4180 J $kg^{-1}\ K^{-1}$), ρ_a is density of air (1.246 kg m^{-3}) and C_a is specific heat capacity of air (1005 J $kg^{-1}\ K^{-1}$). Since the substrate was a homogenous mix of materials (cf. Section 2.1), we consider the given constants to not change with substrate depth.

Q_G was calculated by:

$$Q_G = Q_{G\ HFP} + \Delta Q_S \quad (3)$$

Evapotranspiration rates (ET, in mm s^{-1}) were calculated by, first, filling Q_E data gaps using the REddyProc tool (Reichstein et al., 2005) and, second, applying (Henderson-Sellers, 1984):

$$ET = \frac{Q_E}{\lambda^*(\rho_w/1000)} = \frac{Q_E}{1918.46 * \left(\frac{T_A}{T_A-33.91}\right)^2 * (\rho_w/1000)} \quad (4)$$

where λ is latent heat of vaporization (J kg^{-1}) and T_A is air temperature (K).

To characterize the local climate during the study period and in the long-term (i.e. 1981–2010), hourly meteorological data of a German Weather Service station (Berlin Schönefeld, BSCH) located 1.9 km north-east of the green roof was used.

In order to study green roof-atmosphere exchange under water-limited and well-watered conditions, dry and wet periods were defined. A dry period (DP) is characterized by at least 11 consecutive days with daily precipitation < 1.0 mm. A wet period (WP) is defined by 8 consecutive wet days, which can be interrupted by one dry day (KLIWA, 2006). A wet day is defined, if the linear weighted mean of the previous 7 days is higher than a given threshold value (day 1 has a weight of 0.1, day 7 a weight of 1). The threshold value is given by a sinus function with a period of 365 days, a minimum of 1 mm at the 7th of January, and a maximum of 2 mm at the 7th of July. The remaining periods are defined as intermediate periods (IP).

In terms of urban climate the potential microclimate benefit from green roofs is especially important during hot and sunny weather situations. To examine the functional relationships between water availability and energy exchange during these situations a multiple linear regression model was built using β as response variable and VWC and shortwave downward radiation (K↓) as explanatory variables. Log-log

Please cite this article as: Heusinger, J., Weber, S., Surface energy balance of an extensive green roof as quantified by full year eddy-covariance measurements, Sci Total Environ (2016), http://dx.doi.org/10.1016/j.scitotenv.2016.10.168

transformation was applied in order to achieve normally distributed residuals. The model was established in following data ranges: $0.5 < \beta < 5$, $0.02\ m^3\ m^{-3} < VWC < 0.12\ m^3\ m^{-3}$ and $100\ W\ m^{-2} < K\downarrow < 900\ W\ m^{-2}$. T_A was tested as a further explanatory variable but turned out to be non-significant in the model. Mid-day data of high EC data quality (quality flag = 1, cf. Section 2.4) at 13 CET for the months May to Sep. was used in model building ($n = 61$), which defines the time of the approximate maximum of heat fluxes Q_H and Q_E. Linear regression was applied to study the relationship between Q_H/Q^*, Q_E/Q^* and Q_G/Q^* with VWC and gLAI, respectively.

2.4. EC quality assurance and quality control

For post-processing of the 10 Hz EC raw data, the software EddyPro Version 5.1.1 was used. Double coordinate rotation, WPL (Webb et al., 1980) and spectral corrections (Moncrieff et al., 1997; Moncrieff et al., 2004) were applied. Output flux data (30 min mean values) with quality flag values >6 were rejected according to recommendations by Foken et al. (2004). Flux data from wind directions 36°–54° were excluded since this corresponds to > ± 171° of the azimuth angle (225°) of the CSAT3 anemometer, which is the wind sector influenced by instrument generated flow distortion (Foken, 2016). Periods with precipitation and during which the leaf wetness sensor signalled wet periods (>300 mV) were excluded. In order to detect physically implausible high or low values in the half-hourly flux data we used a spike detection algorithm. For that purpose, a 3-point moving average and standard deviation from the mean diurnal course of each month were calculated. Single data values that deviated from the mean diurnal course with more than ±4 times the standard deviation were rejected. In total, 121 Q_E values (0.6% of data) but none Q_H values were marked as spikes and excluded. After application of all filter criteria 66% of Q_H data and 63% of Q_E data were subject to further analysis.

We conducted spectral analysis to determine whether the scalars of interest deviated from reference functions under ideal (homogenous) conditions. Additionally, spectral characteristics in different wind sectors were analysed. Thus, unstable periods (i.e. $\varsigma < 0$) with well-developed turbulence were selected

$$\varsigma = \frac{z-d}{L} \tag{5}$$

where z is measurement height (m), d is displacement height (m) and L is the Obukhov Length (m). Furthermore, only data with $1.5\ m\ s^{-1} <$ horizontal wind velocity (u) $< 4.0\ m\ s^{-1}$ were used and the wind sector 36°-54° was excluded here as well. Integral turbulence characteristics were studied using Monin-Obukhov similarity theory (MOST) and compared to reference values

$$\frac{\sigma_i}{u^*} = a_i(1 + b_i|\varsigma|)^{1/3} \tag{6}$$

where σ_i is the standard deviation of the scalar of interest (i), u* is friction velocity ($m\ s^{-1}$) and a and b are empirical coefficients.

The flux footprint was calculated for each half-hourly value according to the model of Kormann and Meixner (2001). The mean flux footprint was calculated separately for daytime and nocturnal periods. Nocturnal and daytime hours were classified by K↓, i.e. daytime is defined for time periods with K↓ > 0.

3. Results

3.1. Meteorological characterisation of the study period

Mild winters and temperate summer temperatures (Koeppen climate Cfb) characterize the climate at the BER green roof study site. For the long-term period from 1981 to 2010 a mean annual T_A of 9.3 °C and an annual precipitation sum (P) of 525 mm is documented at BSCH. During the study period from September 2014 to August 2015 mean annual T_A were 1.6 K higher in comparison to the long-term mean (Fig. 2). During the course of the study period 17 hot days (daily $T_{A\ max} > 30$ °C) and 48 summer days (daily $T_{A\ max} > 25$ °C) were observed. In contrast, an average of 9 hot days and 44 summer days per year occurred during the 1981–2010 period.

The study period P sum of 391 mm was 25% lower than the long-term average of 525 mm at BSCH. Except for January 2015 and July 2015 the monthly P was persistently lower than the long-term monthly estimate. The difference was pronounced in May, June and August 2015 with only 46% of the 1981–2010 mean (Fig. 2).

3.2. Seasonal variation of leaf area index

Vegetation coverage of the green roof was rather constant throughout the study period with an average value of 0.40 ± 0.13 (±standard deviation, Fig. 3a). For the relationship between green fraction and gLAI a linear correlation with a coefficient of determination of $R^2 = 0.87$ was observed (Fig. S2). The maximum gLAI of 5.8 represents a sample spot that was fully covered with Sedum, whereas other spots had lower coverages with mixtures of grasses and Sedum species.

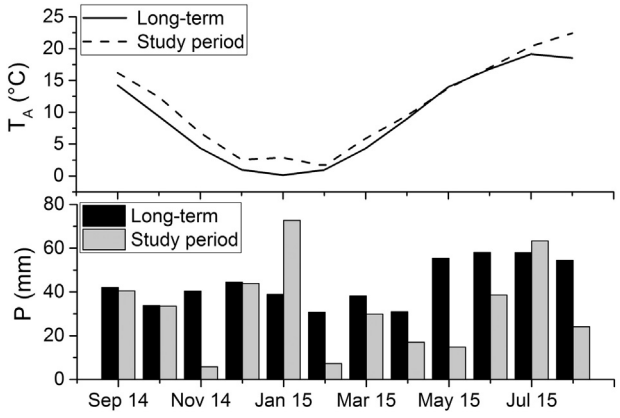

Fig. 2. Mean monthly air temperature (T_A) and precipitation sum (P) during the measurement period and for the German weather service station BSCH (climate normal period 1981–2010).

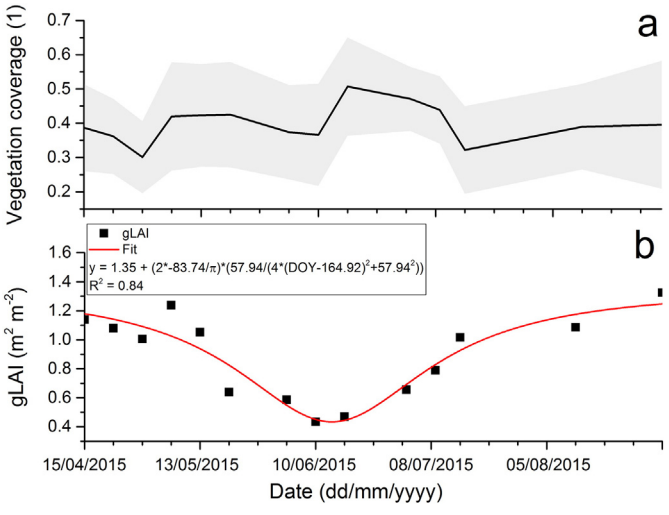

Fig. 3. (a) Variation of mean vegetation coverage and standard deviations (grey shading). (b) Temporal variation of gLAI from Apr. 2015 to Sep. 2015. Black squares are measured values, the fitted curve is a Lorentzian peak function used as smoothing function (with the day of year DOY as independent variable).

Please cite this article as: Heusinger, J., Weber, S., Surface energy balance of an extensive green roof as quantified by full year eddy-covariance measurements, Sci Total Environ (2016), http://dx.doi.org/10.1016/j.scitotenv.2016.10.168

The temporal evolution of gLAI is characterized by a considerable decline between 13 May 2015 and 20 May 2015 (Fig. 3b). In this period plant water availability dropped below the wilting point (i.e. water is left in fine pores but not accessible for plant roots), so that plants were under water stress (Fig. S1b). Around 10 June 2015 the vegetation began to recover until similar gLAI values as compared to the start of the study period were reached. However, some herbaceous plants were not able to recover and replaced by more drought-tolerant *Sedum* species, indicating high interspecific dynamics due to harsh conditions.

3.3. Green roof surface-atmosphere exchange

3.3.1. Spectral analysis and integral turbulence characteristics

The analysis of spectral and integral turbulence characteristics is a central aspect of the quality assurance procedure in EC measurements. The overall shape and location of the spectral energy maximum is similar for all wind direction sectors (Fig. 4a, b). Hence, no additional wind sectors are discarded from further data analysis due to suspicious data (c.f. Section 2.4). The deviation of the −2/3 slope (Kaimal et al., 1972) in the inertial subrange indicates high frequency flux contributions of small eddies which cannot be resolved by the 10 Hz measurement frequency. These high frequency losses were accounted for by the spectral correction procedure according to Moncrieff et al. (1997). The curve of the spectral energy and the location of the spectral energy maximum of the vertical wind velocity fluctuations (w′) as well as the cospectral densities are in agreement with surface layer reference spectra from homogeneous terrain (e.g. Anderson and Verma, 1985; Højstrup, 1981; Fig. 4c, d and e).

The average value of the standard deviation of the vertical wind speed (σ_w) divided by u*, amounts to 1.33. This agrees with the value

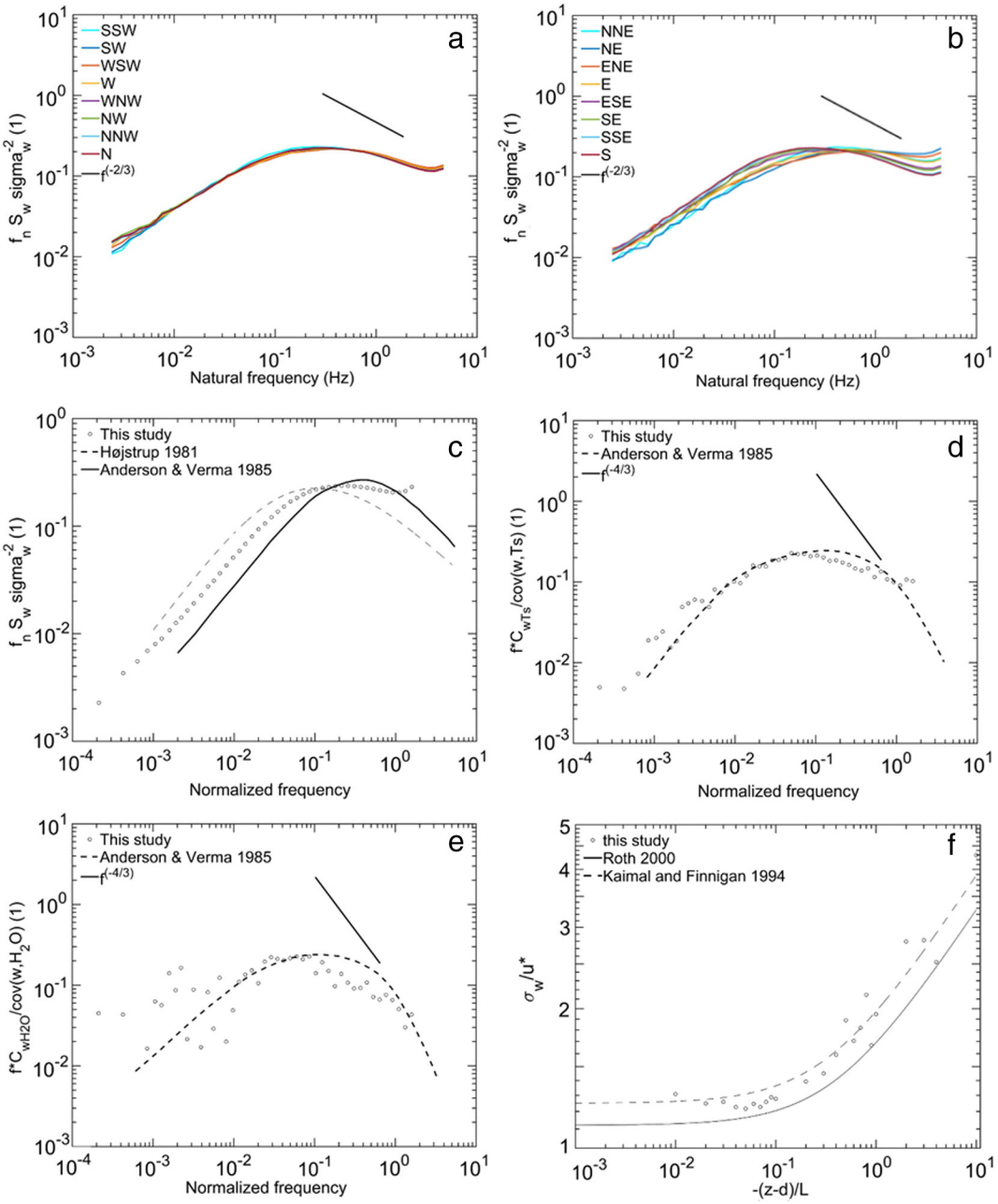

Fig. 4. (a, b) Spectrum of vertical wind vector (w) normalized by its variance for 16 wind direction sectors. The power law of $f^{(-2/3)}$ and $f^{(-4/3)}$ as given by Kolmogorov is depicted as black line. (c) Spectrum of vertical wind vector (w) compared to rural reference spectra by Højstrup (1981) and Anderson and Verma (1985). (d) Cospectrum of w and sonic temperature (T_s). (e) Cospectrum of w and H_2O and (f) dependence of σ_w/u^* on stability parameter $\varsigma = (z - d) / L$ for data of this study compared to reference functions given in Roth (2000) and Panofsky and Dutton (1984).

Please cite this article as: Heusinger, J., Weber, S., Surface energy balance of an extensive green roof as quantified by full year eddy-covariance measurements, Sci Total Environ (2016), http://dx.doi.org/10.1016/j.scitotenv.2016.10.168

of 1.25, which is indicative for undisturbed flow in MOST (Roth, 2000). This also holds for the dependence of σ_w/u^* with increasing instability (Fig. 4f). The data measured at the study site illustrates characteristics of a homogeneous (e.g. Kaimal and Finnigan, 1994) rather than an urban site (Roth, 2000). Using coefficient values for σ_w/u^* from homogeneous terrain (i.e. a = 1.25, b = 3, cf. Eq. (6), Kaimal and Finnigan, 1994) explains the variation of measured values with $R^2 = 0.95$.

The KM footprint model was used to study how well the EC data represents the green roof-atmosphere exchange. On average the daytime 70% flux footprint isoline is located within the boundaries of the green roof (Fig. 5a). The footprint length varies with atmospheric conditions and wind direction. For the two main wind directions sectors NE/E (40°–80°) and SW/W (210°–280°) the average flux footprint (day and night-time) is almost entirely within the green roof fetch (Fig. 5b and c). The nocturnal footprint is larger due to a higher amount of stable situations. We tested for variation in flux data in cases footprint/fetch >1 but did not find significant influence from non-roof source areas.

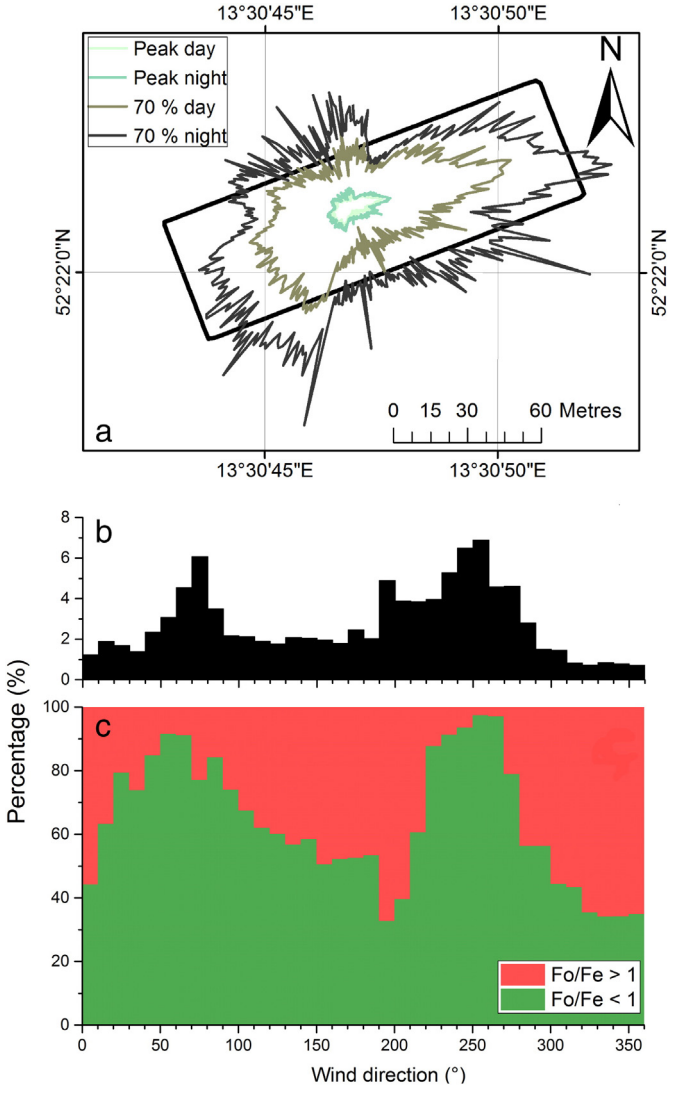

Fig. 5. (a) Average daytime and night-time flux footprint calculated with Kormann and Meixner (2001) footprint model for the entire measurement period. The black rectangle depicts the dimensions of the green roof. (b) Wind frequency distribution binned into 10°-classes. (c) Frequency distribution of the average 70% footprint/fetch ratio (Fo/Fe; daytime and night-time). (For interpretation of the references to colour in this figure legend, the reader is referred to the web version of this article.)

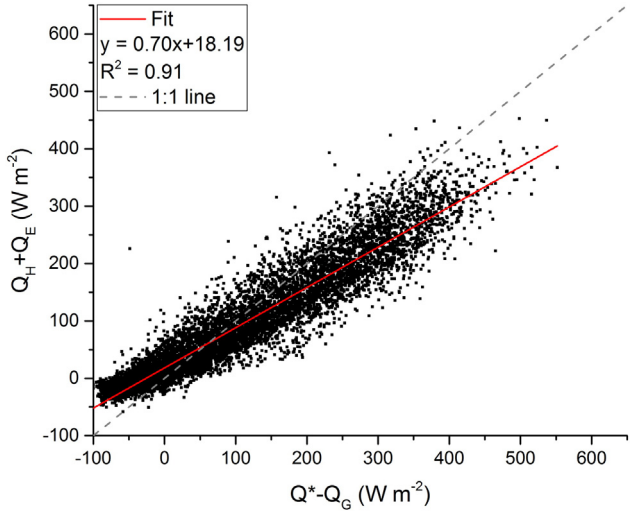

Fig. 6. Relation between the sum of turbulent heat fluxes ($Q_H + Q_E$) and available energy ($Rn - Q_G$). The 1:1 line is depicted as dashed line.

From application of the EC method it is known that the sum of the measured turbulent heat fluxes is typically lower than available energy, which is net radiation (Q^*) subtracted by Q_G. Usually, the so-called energy balance closure gap is quantified by the regression between turbulent heat fluxes and available energy. The energy balance closure in this study is 70% (Fig. 6).

3.3.2. Surface energy balance

The daytime average Q^* during the study period is 169 W m^{-2} whereas the nocturnal average is −47 W m^{-2} (Table 2). The latter is complemented by negative Q_H and Q_G on average, whereas Q_E stays slightly positive at night. The green roof energy exchange is dominated by turbulent heat fluxes Q_H and Q_E in comparison to Q_G. The maximum of Q_H and Q_E during the study period is 386 W m^{-2} and 222 W m^{-2}, respectively. Mean daytime values are 74 W m^{-2} (Q_H) and 38 W m^{-2} (Q_E). Q_G contributes to the energy balance with average daytime values of 22 W m^{-2}. Mean daily totals of Q_G were slightly negative with −0.07 MJ m^{-2} d^{-1}, because Q_G was negative during 63% of the study period and therefore overcompensating higher positive fluxes at daytime.

The average β for the study period is β = 1.0, but increases to β > 1 during MAM (β = 1.5) and JJA (β = 2.0, based on mean daily totals).

Table 2
Energy balance terms for the seasons of the study period (SON, DJF, MAM, JJA), the study period (Year), dry periods (DP), wet periods (WP) and intermediate periods (IP) in terms of mean daily totals given in MJ m^{-2} d^{-1} (Q^*, Q_H, Q_E, Q_G), mean values at daytime (10–16 CET; day) given in W m^{-2}, mean values at nighttime (22–04 CET; night), as β (1) and ET (mm d^{-1}).

	SON	DJF	MAM	JJA	Year	DP	WP	IP
Q^*	1.22	−0.99	4.17	7.53	3.05	2.78	1.55	4.49
Q^* (day)	114	40	218	299	169	172	96	204
Q^* (night)	−36	−34	−62	−54	−47	−52	−35	−46
Q_H	0.23	−1.25	2.48	4.59	1.55	1.93	−0.71	2.18
Q_H (day)	33	−3	106	159	74	85	15	91
Q_H (night)	−12	−19	−20	−14	−16	−15	−25	−16
Q_E	1.32	1.1	1.66	2.27	1.61	1.15	2.69	2.14
Q_E (day)	36	21	43	53	38	29	53	52
Q_E (night)	5	9	5	6	6	4	18	7
Q_G	−0.16	−0.12	−0.07	0.05	−0.07	−0.15	−0.11	−0.03
Q_G (day)	19	4	30	36	22	24	13	26
Q_G (night)	−12	−4	−20	−23	−15	−15	−11	−17
β	0.17	−1.13	1.45	2.03	0.96	1.68	−0.26	1.02
β (day)	1.08	−0.13	2.45	3	1.94	2.95	0.29	1.74
β (night)	−2.61	−2.13	−4.10	−2.15	−2.60	−4.13	−1.38	−2.37
ET	0.64	0.53	0.82	1.11	0.78	0.55	1.29	1.03

Please cite this article as: Heusinger, J., Weber, S., Surface energy balance of an extensive green roof as quantified by full year eddy-covariance measurements, Sci Total Environ (2016), http://dx.doi.org/10.1016/j.scitotenv.2016.10.168

Hence, the dominant fraction of available energy during the warmer times of the year is partitioned into Q_H (Fig. 7). The mean diurnal maximum of Q_H during JJA is 186 W m^{-2}, whereas it is 63 W m^{-2} for Q_E, indicating daytime $\beta = 3.0$ (Fig. 7; Table 2). Because of small precipitation sums β reached about 5 in May, June and August 2015 (Fig. 8). Q_H usually is negative at night with an average of −16 W m^{-2}, whereas Q_E remains positive with 6 W m^{-2} resulting in negative nocturnal β.

Mean daily ET in the summer season of 2015 were 0.80 mm d^{-1} in June, 1.77 mm d^{-1} in July and 0.76 mm d^{-1} in August, indicating high temporal variation of ET on non-irrigated green roofs. The cumulative ET for the study period is 283.2 mm, which corresponds to 72% of the cumulative P measured at BSCH.

3.3.3. Energy exchange during dry and wet periods

Three wet periods (31 days in total) and 10 dry periods (162 days in total) were classified during the 14-month measurement period (Fig. 9). The maximum VWC was observed during the WP in Jan 2015 with 0.48 m^3 m^{-3} whereas it decreased to values close to 0 m^3 m^{-3} several times during DP. Average daytime β were 0.3 in WP and increased to $\beta = 3$ in DP (Table 2). The DP in late July/August 2015 coincided with several hot days (Fig.9).

VWC significantly changes with the start of either WP (increase) or DP (decrease) and is reflected in substantial modification of energy partitioning. The temporal variation of β during DP is best-fitted by an exponential function (Fig. 10). In the summer season the slope of the function increases and VWC is significantly lower in comparison to the other seasons. This is mainly due to more energy that is available for evapotranspiration. Energy partitioning is strongly shifted towards sensible heat exchange in situations when dry periods concur with hot days, i.e. $T_{max} > 30$ °C, as was the case for DP in late July and August 2015 with a mean daytime $\beta = 10.1$. Overall, nine of 17 hot days were observed during DP.

In the course of the only summer WP (08 to 15 July 2014) VWC increased from virtually 0 m^3 m^{-3} ($\beta = 11$) shortly before the start of the WP to 0.16 m^3 m^{-3} ($\beta = 0.67$) on 9 July 2014 (data not shown here). At this point, the maximum Q_E for the whole measurement period with 292 W m^{-2} was measured. Maximum daily ET occurred on 17 July 2014 with 3.27 mm, which is a threefold increase in comparison to the average JJA value (Table 2).

3.4. Functional relationships

Our results so far specified that smaller fractions of incoming energy are partitioned into latent heat during dry and warm summer conditions, which indicates the green roof to show characteristics more of an urban surface rather than an unsealed rural surface. To examine at which VWC values $\beta < 1$ are to be expected, a multiple regression model was used (cf. Section 2.3). The regression function is given by

$$\log_{10}\beta = -2.02 - 0.94 \cdot \log_{10}\mathrm{VWC} + 0.42 \cdot \log_{10}\mathrm{K}\downarrow \quad (7)$$

here, β is modelled reasonably well in the range of $0.5 < \beta < 5$ with normally distributed residuals, RMSE of 0.78 and $R^2 = 0.68$ (Fig. 11). In summer conditions (i.e. K↓ = 500 W m^{-2}) VWC should be higher than 0.11 m^3 m^{-3} at the present site to keep $\beta < 1$, whereas under high radiation conditions (K↓ = 900 W m^{-2}, $\beta < 1$) VWC should be higher than 0.14 m^3 m^{-3} (Fig. S3).

To study the dependence of normalized surface energy balance terms on VWC and gLAI, linear regression was applied for daily mean values in the gLAI monitoring period (15 April to 31 August 2015, Table 3). A linear relationship between VWC and Q_E/Q^* ($R^2 = 0.59$) as well as VWC and Q_H/Q^* ($R^2 = 0.56$) is documented. The statistical relationship between gLAI and Q_E/Q^* as well as Q_H/Q^* is considerably lower with $R^2 = 0.02$ and 0.05, respectively. The influence of both VWC and gLAI on Q_G/Q^* seems to be limited.

4. Discussion

4.1. Data quality and green roof-atmosphere exchange

The green roof on the car park at BER is built of a porous mesh façade whilst the roof is flat without additional roof structures. This minimizes distortion of the rooftop airflow. The EC measurement approach is a micrometeorological method that quantifies surface-atmosphere exchange fluxes by integrating for a certain surface area on the upwind side of the measurement sensor, the so-called flux footprint. The large size of the roof and minimum flow distortion are therefore beneficial for application of the EC method.

The integral turbulence characteristics at the study site agree well with predicted values of MOST at rural and homogenous sites (Kaimal

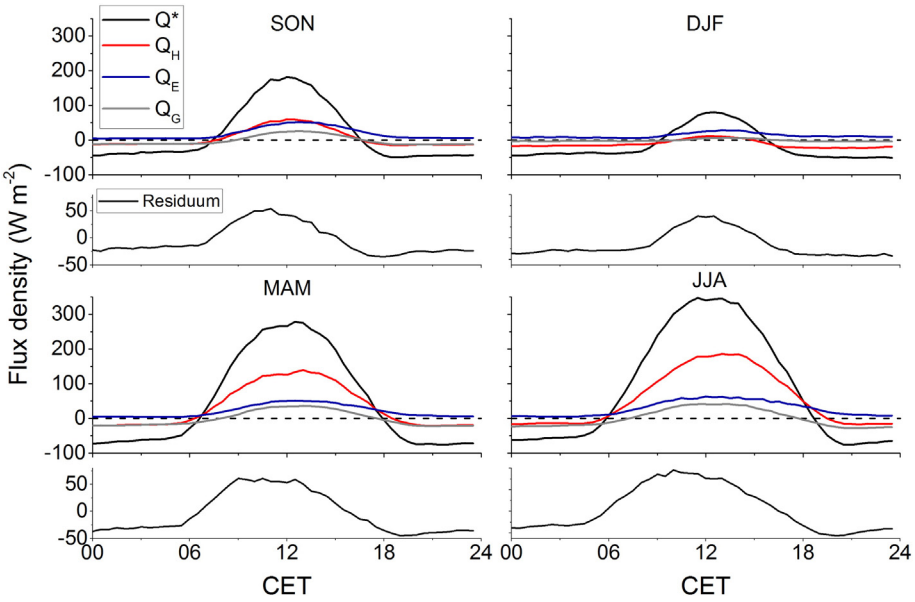

Fig. 7. Mean diurnal courses of the surface energy balance components for the different seasons of the study period (September 2014 to August 2015). The dashed grey line depicts a flux density of 0 W m^{-2}.

Please cite this article as: Heusinger, J., Weber, S., Surface energy balance of an extensive green roof as quantified by full year eddy-covariance measurements, Sci Total Environ (2016), http://dx.doi.org/10.1016/j.scitotenv.2016.10.168

and Finnigan, 1994). Moreover, the spectral energy densities at the green roof site are comparable to rural surface layer reference data (Anderson and Verma, 1985; Højstrup, 1981). The average 70% daytime footprint isoline is almost completely located on the green roof surface according to the KM analytic footprint model (cf. Section 3.3.1). Hence, the time period representing the main exchange of energy

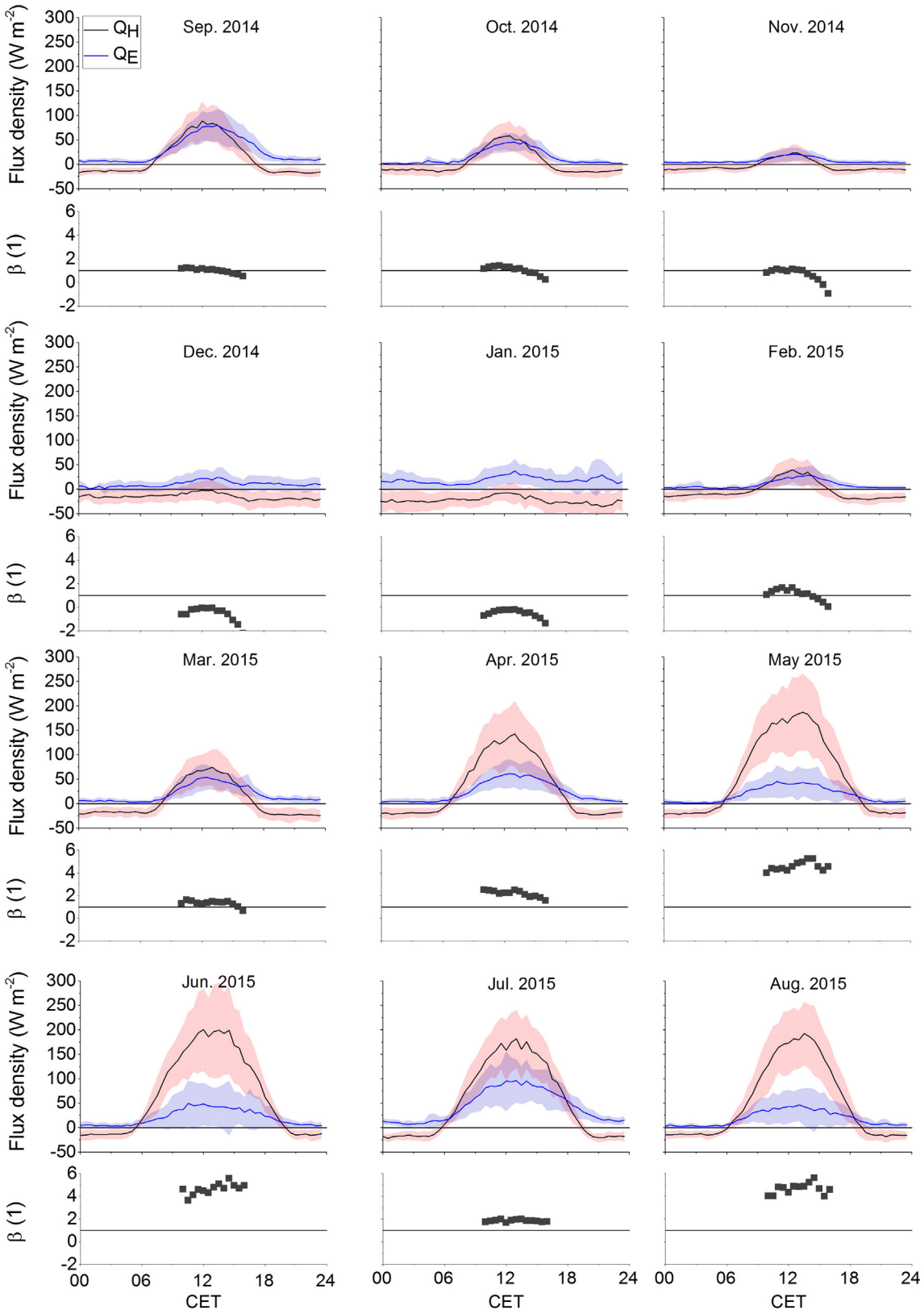

Fig. 8. Monthly mean diurnal courses of Q_H, Q_E and the Bowen ratio during the study period. Standard deviations are depicted by red (Q_H) and blue (Q_E) shadings. The Bowen ratio is depicted for daytime hours between 10:00 h and 16:00 h CET. For reasons of clarity the horizontal black line indicates $\beta = 1$. (For interpretation of the references to colour in this figure legend, the reader is referred to the web version of this article.)

Please cite this article as: Heusinger, J., Weber, S., Surface energy balance of an extensive green roof as quantified by full year eddy-covariance measurements, Sci Total Environ (2016), http://dx.doi.org/10.1016/j.scitotenv.2016.10.168

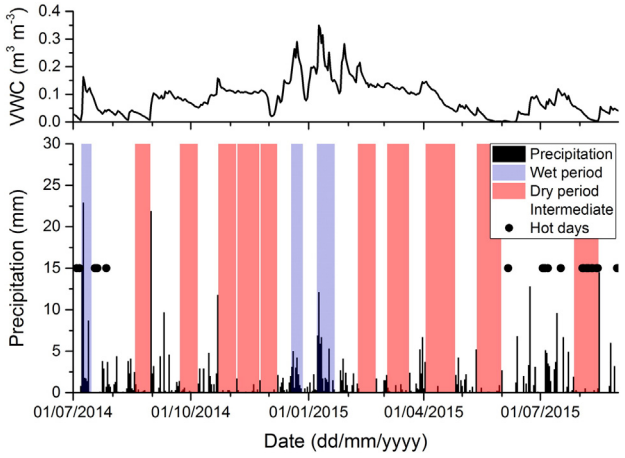

Fig. 9. Dry and wet periods, precipitation and VWC (daily mean) during the measurement period from 01.07.2014 until 31.08.2015. Hot days (T_{max} > 30 °C) are marked with a filled black circle.

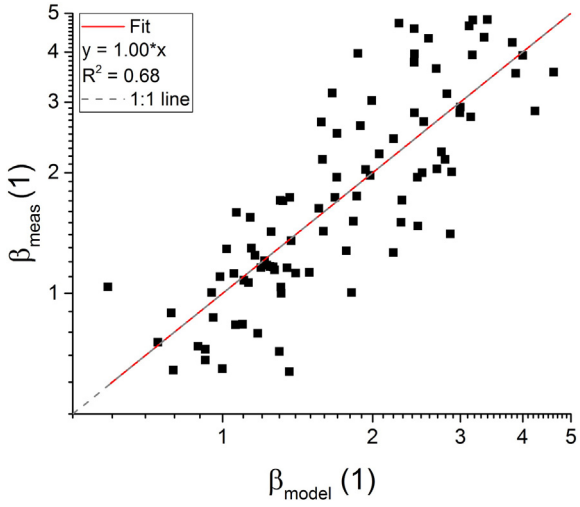

Fig. 11. Scatterplot of modelled (β_{model}) and measured mid-day β (β_{meas}).

(daytime) is well covered by the flux footprint. Significant variation of energy fluxes in cases the footprint was not completely situated on the green roof surface was not observed. A recent comparison between the large eddy simulation (LES) model PALM and KM model illustrates, that the KM model rather overestimates the flux footprint in cases the sensor is located close to a roof surface (Hellsten et al., 2015). However, the application of LES models for footprint estimation of each 30 min flux average is computationally not feasible, yet.

The incomplete energy balance closure of EC measurements is an unsolved issue for which different reasons are under debate (Foken, 2008; Foken et al., 2011; Stoy et al., 2013). However, as discussed by Foken et al. (2011) an unclosed energy balance cannot be taken as a measure of EC data quality. The energy balance closure at the green roof site is in agreement with closure values reported by others. Two studies analysing a large data set from different landscapes within the global flux network FLUXNET conclude that the average energy balance closure at tundra, savanna, grassland, agricultural and forest sites is 79% (±10%, 22 sites studied in Wilson et al., 2002) and 84% (±20%, 173 sites studied in Stoy et al., 2013), respectively. However, the closure estimates considerably vary between study sites, i.e. from 53% to 99% (Wilson et al., 2002). Thus, the energy balance closure of 70% for the present study is a typical result for EC studies.

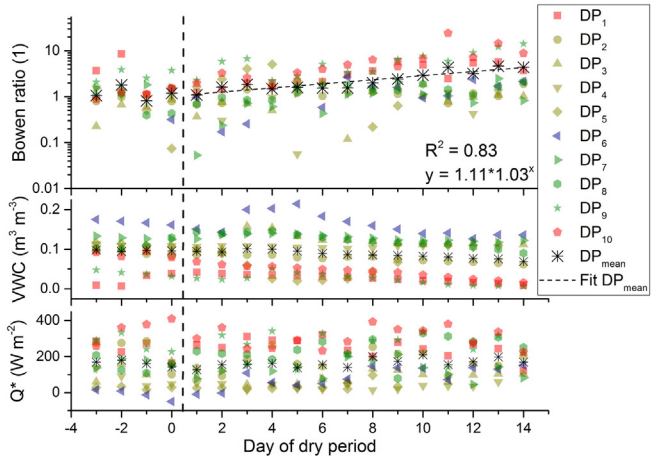

Fig. 10. Mean daytime β, VWC and Q* during the dry periods 1–10. DP_{mean} is the average β of the 10 DP. The seasonal variation is colour-coded (SON = yellow; DJF = blue; MAM = green; JJA = red). A fit (not shown) for DP_{JJA} gives $y = 1.15*1.47^{x}$ with $R^2 = 0.80$. (For interpretation of the references to colour in this figure legend, the reader is referred to the web version of this article.)

Given the results of spectral and integral turbulence characteristics and the favourable conditions of roof size (i.e. footprint) we conclude that the EC flux measurements represent the green roof surface-atmosphere exchange, are comparable with surface layer reference data, are of good quality, and provide an excellent opportunity to validate green roof models.

4.2. Surface energy balance

The turbulent heat fluxes Q_H and Q_E dominate the green roof energy balance throughout the study period compared to Q_G. Substrate heat fluxes are positive by day (22 W m^{-2}) and negative during night (−15 W m^{-2}). Negative fluxes slightly overcompensate positive fluxes due to a higher occurrence during the study period. Hence, the mean daily total of Q_G is slightly negative (−0.07 MJ m^{-2} d^{-1}). In the nocturnal period β turns negative, due to negative Q_H and positive Q_E. As this is complemented by negative nocturnal Q_G and Q* it indicates an important cooling potential of the green roof surface after sunset. This is similar to a field study conducted on an extensive green roof in Braunschweig, Germany (Heusinger and Weber, 2015). Green roofs may therefore exert a cooling effect at times the UHI is most prominent (Oke, 1982).

In summer the energy balance is characterized by high average daytime β values of up to 3 in the summer season. However, during the summer season the green roof is capable to theoretically reduce heating of the near-surface urban atmosphere by 2.3 MJ m^{-2} day^{-1} on average due to evapotranspirative cooling. During the measurements, we observed 10 DP during which VWC declined constantly. Mean daytime β tends to increase exponentially during DP. During and several days after the only WP in summer β values remained <1. Similar observations are reported from chamber flux measurements at an extensive green roof showing β > 4 that dropped to <1 after irrigation (Coutts et al., 2013). In light of these data, β values between 0.12 and 0.35 that were assumed in green roof models seem to be reasonable for non-irrigated green roofs during wet periods but not in hot and dry summer

Table 3
Results of linear regression (y = slope*x + intercept) between gLAI, VWC (independent variable) and energy balance terms (dependent variable) normalized by net radiation Q_E/Q^*, Q_H/Q^*, Q_G/Q^*, respectively.

	Q_H/Q^*			Q_E/Q^*			Q_G/Q^*		
	R^2	Slope	Intercept	R^2	Slope	Intercept	R^2	Slope	Intercept
VWC	0.56	−4.0	0.8	0.59	3.8	0.1	0.00	−0.1	0.1
gLAI	0.05	−0.2	0.7	0.02	0.1	0.1	0.01	0.0	0.1

Please cite this article as: Heusinger, J., Weber, S., Surface energy balance of an extensive green roof as quantified by full year eddy-covariance measurements, Sci Total Environ (2016), http://dx.doi.org/10.1016/j.scitotenv.2016.10.168

conditions (Gaffin et al., 2006; Martens et al., 2008). The present study period was characterized by summer conditions that were somewhat drier than the long term average (cf. Section 3.1). In wetter years, we expect energy partitioning to shift towards characteristics as observed during WP.

The maximum daily ET of 3.3 mm agrees with other green roof studies reporting maximum ET values between 1.7 and 11.4 mm day^{-1} with a median of 3 ± 3.9 mm day^{-1} (DiGiovanni et al., 2012; Marasco et al., 2015; Sherrard and Jacobs, 2011; Voyde et al., 2010; Wolf and Lundholm, 2008). Maximum ET is in the range of grassland EC estimates from temperate sites with maxima between 3 and 5.5 mm day^{-1} (e.g. Novick et al., 2004). It should be noted that the BER green roof is not completely covered by plants, i.e. plant coverage is about 40%. Although comparison data from other green roofs is missing, we assume that lots of extensive green roofs are characterized by higher plant coverages. Therefore, energy partitioning and ET estimates of green roofs might differ as a function of plant coverage. The present green roof, however, was mainly chosen due to its suitability for EC studies (i.e. large roof area) and is believed to be not significantly different from other green roof sites in terms of energy exchange.

4.3. Functional relationships

Our measurements indicate that the water availability of an extensive green roof can be very low in hot summer conditions and drop below the wilting point of herbaceous plants. As a result, low ET rates occur at times when evapotranspiration is needed most to cool the urban atmosphere. We demonstrated that β is mainly dependent on VWC and K↓. Particularly, in summer VWC must be kept above a certain threshold to have mid-day $\beta < 1$, i.e. VWC > 0.11 $m^3\ m^{-3}$ and >0.14 $m^3\ m^{-3}$ for $K\downarrow = 500\ W\ m^{-2}$ and 900 W m^{-2}, respectively. This agrees with Tabares-Velasco and Srebric (2011) who found high and constant ET for VWC values above 0.14 $m^3\ m^{-3}$ in laboratory experiments. In contrast to VWC, the influence of gLAI on Q_E seems to be limited based on findings from regression analysis (cf. Section 3.4). However, the difference between minimum and maximum gLAI during the measurement period was 0.7 $m^2\ m^{-2}$ and might be too small to observe a clear influence on Q_E. Additionally, a larger number of gLAI measurement locations might be necessary to confirm a robust relationship with ET. Voyde et al. (2010) show that green roof plant transpiration is enhanced during well-watered conditions. However, some days after a rainfall event ET was not significantly different between a bare substrate and a vegetated roof plot (Voyde et al., 2010). Thus, optimising ET rates by enhancing green roof LAI might only be valid under well-watered conditions.

Using irrigation to enhance the ecosystem service of green roofs in terms of microclimate regulation might result in a typical trade-off situation. Irrigation is in conflict with efforts to reduce water consumption in (arid) urban areas. Moreover, it might limit retention capability during heavy rainfalls (Van Mechelen et al., 2015). Thus, water should be supplied at an accurate rate to keep VWC above the wilting point under given meteorological conditions and at an enhanced rate during hot, high insolation periods.

5. Conclusions

This study analyses EC measurements of the surface energy balance of an extensive, non-irrigated green roof collected over a period of 14 months. According to the authors knowledge this is the first application of EC on a green roof site. Given the results of the spectral and integral turbulence characteristics as well as the flux footprint analysis we document that the measured energy balance data is of high quality and represents the atmosphere-surface exchange of the green roof.

In comparison to substrate heat flux the green roof surface energy balance was clearly dominated by turbulent heat fluxes. The Bowen ratio was slightly smaller than unity on average but highly variable due to ambient meteorology (energy input) and substrate water availability. Summer β increases to 2 on average but hits a mean daytime β of 10.1 when hot days concur with DP. This is comparable to sealed urban sites rather than rural sites. In contrast, mean daytime β is 0.3 during WP. Following the WP in July 2014 the maximum daily ET of 3.3 mm for the entire measurement period was observed, which is a threefold increase with respect to the average summer season. By means of regression analysis we found, that in summer periods VWC has to be above a certain threshold to have mid-day $\beta < 1$, i.e. VWC > 0.11 $m^3\ m^{-3}$ and >0.14 $m^3\ m^{-3}$ for $K\downarrow = 500\ W\ m^{-2}$ and $K\downarrow = 900\ W\ m^{-2}$, respectively. In contrast to VWC, gLAI seems to be of minor importance for variation of Q_E at the present site. Negative nocturnal Q_H and Q^* demonstrate a considerable cooling potential of the green roof, at times the UHI is most significant.

Urban green roofs are considered as one important measure to tackle both urban warming and the impact of climate change on thermal urban climate. However, in dry and hot daytime conditions (i.e. at times when evaporative cooling by urban green is most important) non-irrigated extensive green roofs tend to show characteristics, namely Bowen ratios that correspond to typical sealed urban estimates. Our results indicate that the microclimate benefit of common non-irrigated urban green roofs can be significantly optimised by using sustainable irrigation approaches. Given the likelihood of increasing duration and intensity of future heat waves this is an important aspect of roof greening. As urban green roofs comprise a range of different properties (plant types, coverage, maintenance, and substrate) further comparative studies of green roof benefits in terms of the energy balance of irrigated versus non-irrigated green roofs by state-of-the-art measurements and modelling are recommended.

Acknowledgements

We thank Jochen Heimberg (Environment Department, Berlin Brandenburg Airport) for permission to use the green roof site for EC measurements. Thanks to Hagen Mittendorf (Climatology and Environmetal Meteorology working group, TU Braunschweig) for EC station maintenance as well as to Sascha Iden and Tobias Weber from the Soil Science and Soil Physics group at the Institute of Geoecology, TU Braunschweig for conducting laboratory analysis of the green roof substrate. We also thank the two anonymous reviewers for their constructive critics on the earlier version of the manuscript.

Appendix A. Supplementary data

Supplementary data to this article can be found online at http://dx.doi.org/10.1016/j.scitotenv.2016.10.168.

References

Anderson, D.E., Verma, S.B., 1985. Turbulence spectra of CO_2, water vapor, temperature and wind velocity fluctuations over a crop surface. Bound.-Layer Meteorol. 33 (1), 1–14.

Ansel, W., Zeidler, J., Esch, T., 2015. Fernerkundliche Identifizierung von Vegetationsflächen auf Dächern zur Entwicklung des für die Bereiche des Stadtklimas, der Stadtentwässerung und des Artenschutzes aktivierbaren Flächenpotenzials in Städten. Deutscher Dachgärtner Verband e.V. (46 pp).

Ayata, T., Tabares-Velasco, P.C., Srebric, J., 2011. An investigation of sensible heat fluxes at a green roof in a laboratory setup. Build. Environ. 46 (9), 1851–1861.

Baldocchi, D., 2014. Measuring fluxes of trace gases and energy between ecosystems and the atmosphere–the state and future of the eddy covariance method. Glob. Chang. Biol. 20 (12), 3600–3609.

Berndtsson, J.C., 2010. Green roof performance towards management of runoff water quantity and quality: a review. Ecol. Eng. 36 (4), 351–360.

Bowler, D.E., Buyung-Ali, L., Knight, T.M., Pullin, A.S., 2010. Urban greening to cool towns and cities: a systematic review of the empirical evidence. Landsc. Urban Plan. 97 (3), 147–155.

Chow, W.T., Volo, T.J., Vivoni, E.R., Jenerette, G.D., Ruddell, B.L., 2014. Seasonal dynamics of a suburban energy balance in Phoenix, Arizona. Int. J. Climatol. 34 (15), 3863–3880.

Christen, A., Vogt, R., 2004. Energy and radiation balance of a central European city. Int. J. Climatol. 24 (11), 1395–1421.

Coutts, C., Hahn, M., 2015. Green infrastructure, ecosystem services, and human health. Int. J. Environ. Res. Public Health 12 (8), 9768–9798.

Coutts, A.M., Beringer, J., Tapper, N.J., 2007. Impact of increasing urban density on local climate: spatial and temporal variations in the surface energy balance in Melbourne, Australia. J. Appl. Meteorol. Climatol. 46 (4), 477–493.

Coutts, A.M., Daly, E., Beringer, J., Tapper, N.J., 2013. Assessing practical measures to reduce urban heat: green and cool roofs. Build. Environ. 70, 266–276.

Derkzen, M.L., Teeffelen, A.J., Verburg, P.H., 2015. REVIEW: quantifying urban ecosystem services based on high-resolution data of urban green space: an assessment for Rotterdam, the Netherlands. J. Appl. Ecol. 52 (4), 1020–1032.

DiGiovanni, K., Montalto, F., Gaffin, S., Rosenzweig, C., 2012. Applicability of classical predictive equations for the estimation of evapotranspiration from urban green spaces: green roof results. J. Hydrol. Eng. 18 (1), 99–107.

Foken, T., 2008. The energy balance closure problem: an overview. Ecol. Appl. 18 (6), 1351–1367.

Foken, T., 2016. Angewandte Meteorologie: Mikrometeorologische Methoden. Springer Spektrum, Berlin; Heidelberg (394 p).

Foken, T., Göckede, M., Mauder, M., Mahrt, L., Amiro, B., Munger, W., 2004. Post-field data quality control. Handbook of Micrometeorology. Springer Netherlands, pp. 181–208.

Foken, T., Aubinet, M., Finnigan, J.J., Leclerc, M.Y., Mauder, M., Paw, K.T.U., 2011. Results of a panel discussion about the energy balance closure correction for trace gases. Bull. Am. Meteorol. Soc. 92 (4), ES13.

Gaffin, S., Rosenzweig, C., Parshall, L., Hillel, D., Eichenbaum-Pikser, J., Greenbaum, A., Berghage, R., May 2006. Quantifying evaporative cooling from green roofs and comparison to other land surfaces. Fourth Annual Greening Rooftops for Sustainable Communities Conference, Awards and Trade Show, pp. 11–12.

Garratt, J.R., 1992. The Atmospheric Boundary Layer. Cambridge University Press (316 p).

Goldbach, A., Kuttler, W., 2013. Quantification of turbulent heat fluxes for adaptation strategies within urban planning. Int. J. Climatol. 33 (1), 143–159.

Gómez-Baggethun, E., Gren, Å., Barton, D.N., Langemeyer, J., McPhearson, T., O'Farrell, P., Kremer, P., 2013. Urban ecosystem services. Urbanization, Biodiversity and Ecosystem Services: Challenges and Opportunities. Springer Netherlands, pp. 175–251.

Grimmond, C.S.B., Oke, T.R., 2002. Turbulent heat fluxes in urban areas: observations and a local-scale urban meteorological parameterization scheme (LUMPS). J. Appl. Meteorol. 41 (7), 792–810.

Grimmond, C.S.B., Salmond, J.A., Oke, T.R., Offerle, B., Lemonsu, A., 2004. Flux and turbulence measurements at a densely built-up site in Marseille: heat, mass (water and carbon dioxide), and momentum. J. Geophys. Res. Atmos. 109 (D24).

Haase, D., Larondelle, N., Andersson, E., Artmann, M., Borgström, S., Breuste, J., ... Kabisch, N., 2014. A quantitative review of urban ecosystem service assessments: concepts, models, and implementation. Ambio 43 (4), 413–433.

Hellsten, A., Luukkonen, S.M., Steinfeld, G., Kanani-Sühring, F., Markkanen, T., Järvi, L., ... Raasch, S., 2015. Footprint evaluation for flux and concentration measurements for an urban-like canopy with coupled Lagrangian stochastic and large-eddy simulation models. Bound.-Layer Meteorol. 157 (2), 191–217.

Henderson-Sellers, B., 1984. A new formula for latent heat of vaporization of water as a function of temperature. Q. J. R. Meteorol. Soc. 110 (466), 1186–1190.

Heusinger, J., Weber, S., 2015. Comparative microclimate and dewfall measurements at an urban green roof versus bitumen roof. Build. Environ. 92, 713–723.

Højstrup, J., 1981. A simple model for the adjustment of velocity spectra in unstable conditions downstream of an abrupt change in roughness and heat flux. Bound.-Layer Meteorol. 21 (3), 341–356.

Kaimal, J.C., Finnigan, J.J., 1994. Atmospheric Boundary Layer Flows: Their Structure and Measurement (289 p).

Kaimal, J.C., Wyngaard, J., Izumi, Y., Coté, O.R., 1972. Spectral characteristics of surface-layer turbulence. Q. J. R. Meteorol. Soc. 98 (417), 563–589.

KLIWA, 2006. Langzeitverhalten der Starkniederschläge in Baden-Württemberg und Bayern (93 p).

Kormann, R., Meixner, F.X., 2001. An analytical footprint model for non-neutral stratification. Bound.-Layer Meteorol. 99 (2), 207–224.

Kumar, R., Kaushik, S.C., 2005. Performance evaluation of green roof and shading for thermal protection of buildings. Build. Environ. 40 (11), 1505–1511.

Lee, X., Massman, W., Law, B. (Eds.), 2006. Handbook of micrometeorology: a guide for surface flux measurement and analysis Vol. 29. Springer Science & Business Media (249 p).

Liebethal, C., Huwe, B., Foken, T., 2005. Sensitivity analysis for two ground heat flux calculation approaches. Agric. For. Meteorol. 132 (3), 253–262.

Marasco, D.E., Culligan, P.J., McGillis, W.R., 2015. Evaluation of common evapotranspiration models based on measurements from two extensive green roofs in New York City. Ecol. Eng. 84, 451–462.

Martens, R., Bass, B., Alcazar, S.S., 2008. Roof–envelope ratio impact on green roof energy performance. J. Urban Econ. 11 (4), 399–408.

Mazdiyasni, O., AghaKouchak, A., 2015. Substantial increase in concurrent droughts and heatwaves in the United States. Proc. Natl. Acad. Sci. 112 (37), 11484–11489.

Moncrieff, J.B., Massheder, J.M., De Bruin, H., Elbers, J., Friborg, T., Heusinkveld, B., ... Verhoef, A., 1997. A system to measure surface fluxes of momentum, sensible heat, water vapour and carbon dioxide. J. Hydrol. 188, 589–611.

Moncrieff, J., Clement, R., Finnigan, J., Meyers, T., 2004. Averaging, detrending, and filtering of eddy-covariance time series. Handbook of Micrometeorology. Springer Netherlands, pp. 7–31.

Novick, K.A., Stoy, P.C., Katul, G.G., Ellsworth, D.S., Siqueira, M.B.S., Juang, J., Oren, R., 2004. Carbon dioxide and water vapor exchange in a warm temperate grassland. Oecologia 138 (2), 259–274.

Oberndorfer, E., Lundholm, J., Bass, B., Coffman, R.R., Doshi, H., Dunnett, N., ... Rowe, B., 2007. Green roofs as urban ecosystems: ecological structures, functions, and services. Bioscience 57 (10), 823–833.

Oke, T.R., 1982. The energetic basis of the urban heat island. Q. J. R. Meteorol. Soc. 108 (455), 1–24.

Panofsky, H.A., Dutton, J.A., 1984. Atmospheric turbulence: models and methods for engineering applications (397 pp.).

Pfoser, N., Henrich, J., Jenner, N., Schreiner, J., Kanashiro, C., Heusinger, J., Weber, S., Hegger, M., Dettmar, J., 2014. Gebäude Begrünung Energie - Potenziale und Wechselwirkungen (Buildings, Greening and Energy: Potentials and Interdependencies). Forschungsgesellschaft Landschaftsentwicklung Landschaftsbau e.V. (FLL); Bundesinstitut für Bau-, Stadt- und Raumforschung (BBSR), FLL-Schriftenreihe, FV2014/01, Bonn (305 p).

Reichstein, M., Falge, E., Baldocchi, D., Papale, D., Aubinet, M., Berbigier, P., ... Grünwald, T., 2005. On the separation of net ecosystem exchange into assimilation and ecosystem respiration: review and improved algorithm. Glob. Chang. Biol. 11 (9), 1424–1439.

Richardson, A.D., Jenkins, J.P., Braswell, B.H., Hollinger, D.Y., Ollinger, S.V., Smith, M.L., 2007. Use of digital webcam images to track spring green-up in a deciduous broadleaf forest. Oecologia 152 (2), 323–334.

Roth, M., 2000. Review of atmospheric turbulence over cities. Q. J. R. Meteorol. Soc. 126 (564), 941–990.

Russo, S., Dosio, A., Graversen, R.G., Sillmann, J., Carrao, H., Dunbar, M.B., ... Vogt, J.V., 2014. Magnitude of extreme heat waves in present climate and their projection in a warming world. J. Geophys. Res. Atmos. 119 (22), 500–512.

Sailor, D.J., 2008. A green roof model for building energy simulation programs. Energ. Buildings 40 (8), 1466–1478.

Sailor, D.J., Hutchinson, D., Bokovoy, L., 2008. Thermal property measurements for ecoroof soils common in the western US. Energ. Buildings 40 (7), 1246–1251.

Sailor, D.J., Elley, T.B., Gibson, M., 2011. Exploring the building energy impacts of green roof design decisions–a modeling study of buildings in four distinct climates. J. Build. Phys. 35 (4), 372–391.

Sherrard Jr., J.A., Jacobs, J.M., 2011. Vegetated roof water-balance model: experimental and model results. J. Hydrol. Eng. 17 (8), 858–868.

Smith, K.R., Roebber, P.J., 2011. Green roof mitigation potential for a proxy future climate scenario in Chicago, Illinois. J. Appl. Meteorol. Climatol. 50 (3), 507–522.

Stovin, V., Poë, S., Berretta, C., 2013. A modelling study of long term green roof retention performance. J. Environ. Manag. 131, 206–215.

Stoy, P.C., Mauder, M., Foken, T., Marcolla, B., Boegh, E., Ibrom, A., ... Cescatti, A., 2013. A data-driven analysis of energy balance closure across FLUXNET research sites: the role of landscape scale heterogeneity. Agric. For. Meteorol. 171, 137–152.

Tabares-Velasco, P.C., Srebric, J., 2011. Experimental quantification of heat and mass transfer process through vegetated roof samples in a new laboratory setup. Int. J. Heat Mass Transf. 54 (25), 5149–5162.

Van Mechelen, C., Dutoit, T., Hermy, M., 2015. Adapting green roof irrigation practices for a sustainable future: a review. Sustainable Cities and Society 19, 74–90.

Voyde, E., Fassman, E., Simcock, R., Wells, J., 2010. Quantifying evapotranspiration rates for New Zealand green roofs. J. Hydrol. Eng. 15 (6), 395–403.

Webb, E.K., Pearman, G.I., Leuning, R., 1980. Correction of flux measurements for density effects due to heat and water vapour transfer. Q. J. R. Meteorol. Soc. 106 (447), 85–100.

Weber, S., 2006. Comparison of in-situ measured ground heat fluxes within a heterogeneous urban ballast layer. Theor. Appl. Climatol. 83, 169–179.

Wilson, K., Goldstein, A., Falge, E., Aubinet, M., Baldocchi, D., Berbigier, P., ... Grelle, A., 2002. Energy balance closure at FLUXNET sites. Agric. For. Meteorol. 113 (1), 223–243.

Wolf, D., Lundholm, J.T., 2008. Water uptake in green roof microcosms: effects of plant species and water availability. Ecol. Eng. 33 (2), 179–186.

Yang, J., Yu, Q., Gong, P., 2008. Quantifying air pollution removal by green roofs in Chicago. Atmos. Environ. 42 (31), 7266–7273.

Please cite this article as: Heusinger, J., Weber, S., Surface energy balance of an extensive green roof as quantified by full year eddy-covariance measurements, Sci Total Environ (2016), http://dx.doi.org/10.1016/j.scitotenv.2016.10.168